

Frequency- and time-resolved measurements of FeTaN films with longitudinal bias fields

C. Alexander, Jr.^{a)} and J. Rantschler

*Department of Physics and Astronomy and Center for Materials for Information Technology,
University of Alabama, Tuscaloosa, Alabama 35487*

T. J. Silva and P. Kabos

National Institute for Standards and Technology, Boulder, Colorado 80303

The high frequency characteristics of 100 nm FeTaN films have been studied by using both time-resolved inductive techniques and frequency-resolved permeability measurements. Experiments performed as a function of longitudinal bias fields from 120 to 2400 A/m (1.5–30 Oe) showed precessional frequencies from 1.3 to 2.5 GHz, initial permeabilities from 1600 to 500, and damping constants $\alpha=0.013$ to 0.0045. It is illustrated that the magnetization precessional data obtained from the time-resolved inductive technique can be Fourier transformed to the frequency domain to give the real and imaginary components of a permeability spectrum; this spectrum compares well with data obtained from frequency-resolved permeability measurements. It is also demonstrated that accurate values of the damping constant α can only be determined from permeameters whose bandwidth is two to three times the ferromagnetic resonance frequency of the material to be measured. © 2000 American Institute of Physics. [S0021-8979(00)87808-1]

I. INTRODUCTION

The areal density of hard disk storage systems has been increasing rapidly over the past decade, causing concern about the high frequency performance of the system components.¹ One material that shows good characteristics for a future recording head is FeTaN.^{2–4} We describe the experiments that have been used to characterize the high frequency performance of 100 nm films of FeTaN.

Inductive techniques were used in 1960 by Dietrich, Proebster, and Wolf^{5–7} to measure the switching characteristics of the thin magnetic films, and more recently, Silva *et al.*⁸ have used modern high-speed electronics and broadband inductive techniques to study magnetization dynamics. In this article, it is illustrated that the magnetization precessional data obtained from the time-resolved inductive technique can be Fourier transformed to the frequency domain to give the real and imaginary components of a permeability spectrum; this spectrum compares well with data obtained from frequency-resolved permeability measurements.

II. EXPERIMENTAL DETAILS

The experimental details of the broadband inductive technique are described in detail by Silva *et al.*⁸ For these experiments, a coplanar waveguide was used to produce step magnetic fields of 160 A/m (2 Oe), and longitudinal bias fields from 120 to 2400 A/m (1.5 to 30 Oe) were employed. The bandwidth of this equipment, as determined from the transmitted step rise time, is greater than 6 GHz. For the permeability measurements, a 3-GHz network analyzer was used in conjunction with a permeameter head design similar to that of Yamaguchi *et al.*⁹ The permeameter head had a driving plane width of 3.5 cm, a spacing to the ground plane

of 0.7 cm, and a single turn microstrip pickup coil was employed. The bandwidth of this equipment as determined from an S_{21} parameter measurement is approximately 1.5 GHz. In both sets of experiments, sputtered, 8 mm×8 mm×100 nm samples of FeTaN deposited on glass were used.

III. RESULTS AND DISCUSSION

A permeability measurement requires three frequency sweeps by the network analyzer configured to measure the S_{21} parameters of the sample with a low bias-field $S_{(u)}(f)$, and the sample with a saturation field $S_{(s)}(f)$. These sweeps are stored in a computer and the permeability is calculated from

$$\mu(f) = C \frac{S_u(f) - S_s(f)}{S_s(f)}, \quad (1)$$

where C is a low-frequency calibration factor. The calibration standard is a 44 nm NiFe film whose measured low-frequency permeability is compared to a value calculated from B_s and H_k measurements on a vibrating sample magnetometer (VSM). The calibration factor also takes into account the relative cross-sectional areas of the sample and the reference. An experimental permeability curve for a longitudinal bias field of 880 A/m (11 Oe) is shown as the dotted lines in Fig. 1. As longitudinal bias fields are applied, the initial permeability values ($\omega=0$) decrease, the ferromagnetic resonance (FMR) frequencies increase, and the damping constant decreases. The experimental values of the initial permeability and the resonance frequency are plotted as a function of the applied longitudinal bias field in Fig. 2, and the solid lines represent calculated values based on $B_s = 2$ T and $H_k = 800$ A/m (10 Oe).

^{a)}Electronic mail: calexand@mint.ua.edu

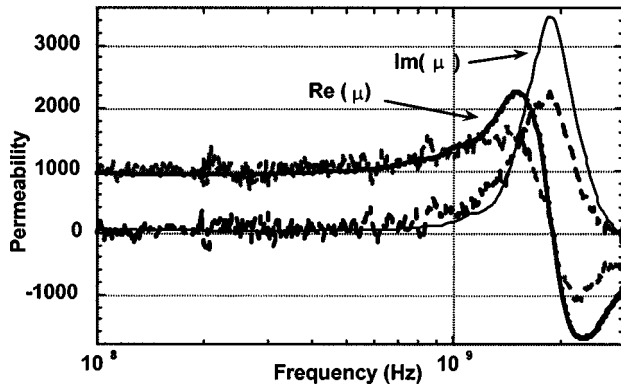


FIG. 1. Real and imaginary components of the permeability of a FeTaN film, measured with a longitudinal bias of 880 A/m (11 Oe). The dotted lines represent the experimental permeameter data, while the solid lines indicate the Fourier transform of the step response data shown in Fig. 3.

A new approach to the permeability measurements of thin ferromagnetic films uses the broadband time-resolved inductive technique.⁸ The use of this technique to measure permeability relies on the fact that there is a linear relation between the time-dependent driving field and the resulting magnetization in the small signal limit, which thereby permits the use of linear superposition in conjunction with Fourier analysis.^{10,11} Following the notation of Ref. 8, the relation between the Fourier transforms of the magnetization and the applied field can be expressed in the form

$$\tilde{M}_y(\omega) = \tilde{\chi}_{yy}(\omega) \tilde{H}_y(z, \omega). \quad (2)$$

Here, $\tilde{\chi}_{yy}(\omega)$ is the diagonal component of the susceptibility tensor in the y -axis direction parallel to the applied field step. The induced voltage is proportional to the time derivative of $M_y(t)$ and, in the frequency domain, can be expressed as

$$\tilde{V}(\omega) = \frac{i\omega\mu_0 A \epsilon}{4} \tilde{M}_y(\omega), \quad (3)$$

where ϵ is the inductive coupling factor and A is the sample's cross-sectional area in the x - z plane. The Fourier transform of the applied field instantaneous step function of amplitude H_0 is

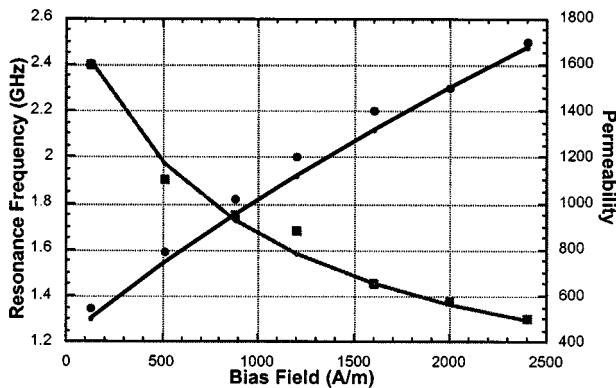


FIG. 2. Experimental ferromagnetic resonance frequencies and initial permeabilities as a function of longitudinal bias fields for FeTaN films.

$$\tilde{H}_y(z, \omega) = \frac{H_0 g(z)}{i\omega}, \quad (4)$$

with $g(z)$ representing the spacing loss of the field due to the distance of the film from the waveguide pickup. By inserting Eqs. (2) and (4) into the induced voltage expression (3), we show that the Fourier transform of the induced voltage is proportional to the susceptibility spectrum.

$$\tilde{V}(\omega) = \frac{1}{4} \mu_0 A H_0 \epsilon g(z) \tilde{\chi}_{yy}(\omega). \quad (5)$$

For the permeability measurements, a system calibration is necessary. From the reciprocity theorem,¹² the inductive coupling factor and the spatial loss factor should be equal, and the dc susceptibility can be related to the material's saturation magnetization M_s and anisotropy for a thin magnetic film magnetized in the plane of the film as

$$\tilde{\chi}_{yy}(\omega=0) = \frac{M_s}{H_b + H_k}, \quad (6)$$

where H_b is the longitudinal bias field. The spatial loss factor $g(z) = \epsilon$ by reciprocity and is related to the zero-frequency Fourier component of the induced voltage and the sample parameters by combining Eqs. (5) and (6) to give

$$g(z) = \sqrt{\frac{4\tilde{V}(\omega=0)(H_b + H_k)}{\mu_0 M_s H_0 A}}. \quad (7)$$

By inserting Eq. (7) into Eq. (5) we get the final, practical relation that defines the permeability

$$\tilde{\chi}_{yy}(\omega) = \frac{\tilde{V}(\omega)}{\tilde{V}(\omega=0)} \frac{M_s}{H_b + H_k}. \quad (8)$$

The computation of $\tilde{\chi}_{yy}(\omega)$ then requires a Fourier transform of the step response $V(t)$ and measurement of the static material parameters. The following caveats should be kept in mind when applying Eq. (8). First, the temporal duration of the time-resolved measurement should be sufficiently long to capture the final equilibrium state of the magnetization. Second, the width of the waveguide employed for the time-resolved measurement cannot be so small that size-related demagnetizing effects inflate the effective value of H_k beyond the dc value obtained with a bulk magnetometer, such as a B - H loop or VSM. Third, the assumption that $g(z)$ and ϵ are independent of frequency is only true in the case that the microwave skin depth is greater than the thickness of the waveguide conductor. Nevertheless, reciprocity and the equivalence of ϵ and $g(z)$ should still be valid in the near-field regime ($l < c/f$) where retardation effects can be ignored, since reciprocity is a general property of Faraday's Law, independent of frequency.¹² Finally, the assumption of linearity can only be true in the limit of sufficiently small driving field H_0 . For example, nonlinear coupling to higher order magnetostatic modes as H_0 approaches H_k can greatly complicate the analysis.⁸

A step response curve for a 100 nm FeTaN film with an 880 A/m (11 Oe) bias field is shown in Fig. 3. The Fourier transformed permeability spectrum for this curve is shown as

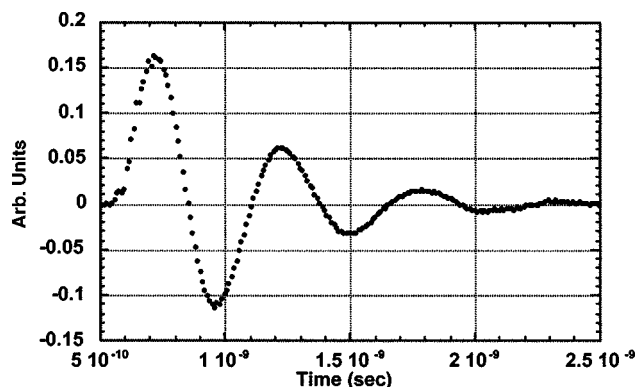


FIG. 3. Experimental data from a step-response measurement of FeTaN films with a longitudinal bias field of 880 A/m (11 Oe).

the solid lines in Fig. 1. It can be seen that the initial permeability and the resonance frequency match the dotted curves from the permeameter, but the shape of the curves near the resonance frequency are quite different. Calculations of the real and imaginary components of the permeability spectrum show that the shape of the curve in this region should be determined primarily by the value of the damping.¹³ The bandwidth of the inductive apparatus (6 GHz) is greater than that of the permeameter (1.5 GHz), so we anticipated that, for frequencies ≥ 1.5 GHz, the frequency-resolved spectrum would be distorted. This was indeed found to be the case as illustrated in Fig. 1. A value of the damping constant α calculated from the frequency-resolved spectrum of Fig. 1 gave a value of 0.014, whereas a value calculated from the Fourier transformed time-resolved data gave a value of 0.0085. The transformed time-domain data can be made to match the frequency-resolved data by applying a 1.5 GHz low-pass filter function; an inverse filter function applied to the frequency-resolved data will reproduce the transformed time-resolved data. We have used the transformed inductive data to derive damping constant values for the FeTaN films from permeability formulas¹³ based on the Landau–Lifshitz–Gilbert equation. The derived values of α are shown in Fig. 4, and combined with the large initial permeability and high resonance frequency, illustrate good high frequency characteristics for FeTaN films. The value of α measured at the highest bias field, 0.0045, is similar to a value, 0.004, measured by FMR at 9.38 GHz.

IV. CONCLUSIONS

Experiments on 100 nm films of FeTaN, performed as a function of longitudinal bias fields from 120 to 2400 A/m (1.5–30 Oe), showed precessional frequencies from 1.3 to 2.5 GHz, initial permeabilities from 1600 to 500, and damping constants $\alpha = 0.013$ to 0.0045. It has been demonstrated

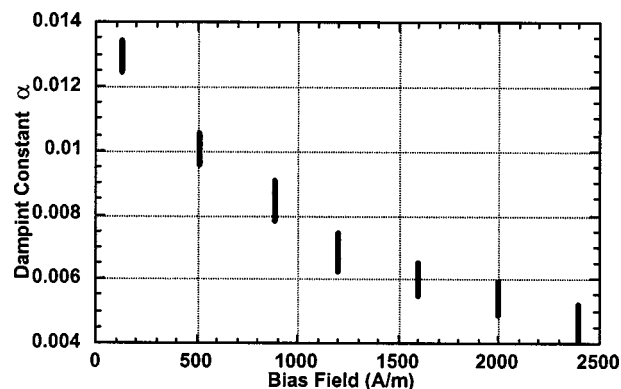


FIG. 4. Values of the damping constant α as a function of longitudinal bias field for FeTaN films.

that high-frequency permeability data can be determined from both time-resolved and frequency-resolved measurements. The Fourier transformation equations used to calculate the real and imaginary components of a permeability spectrum from the time-resolved data have been provided. From comparisons of low-pass filter calculations and high-bandwidth data, it has also been demonstrated that accurate values of the damping constant α can only be determined from data produced by equipment whose bandwidth is two to three times greater than the FMR frequency of the measured material.

ACKNOWLEDGMENTS

This research was supported by NSIC-EHDR Award No. 542417-55139 and made use of the NSF MRSEC Shared facilities Grant No. DMR-98-09423. One of the authors (C. A.) wishes to express his thanks to Charles Rogers, Tom Silva, and Ron Goldfarb for their support during his stay at CU and NIST.

- ¹K. B. Klaassen, R. G. Hirko, and J. T. Contreras, *IEEE Trans. Magn.* **34**, 1822 (1998).
- ²B. Viala, M. K. Minor, and J. A. Barnard, *J. Appl. Phys.* **80**, 3941 (1996).
- ³M. K. Minor and J. A. Barnard, *J. Appl. Phys.* **85**, 4567 (1999).
- ⁴V. R. Inturi and J. A. Barnard, *IEEE Trans. Magn.* **31**, 2660 (1995).
- ⁵W. Dietrich, W. E. Proebster, and P. Wolf, *IBM Journal*, April, 1960, p. 189.
- ⁶W. Dietrich and W. E. Proebster, *J. Appl. Phys.* **31**, 281S (1960).
- ⁷P. Wolf, *J. Appl. Phys.* **32**, 95S (1960).
- ⁸T. J. Silva, C. S. Lee, T. M. Crawford, and C. T. Rogers, *J. Appl. Phys.* **85**, 7849 (1999).
- ⁹M. Yamaguchi, S. Yabukami, and K. I. Arai, *IEEE Trans. Magn.* **33**, 3619 (1997).
- ¹⁰J. Baker-Jarvis, *Smart Mater. Struct.* **2**, 113 (1993).
- ¹¹W. T. Grandy, Jr., *Foundations of Statistical Mechanics*, Vol. II (Reidel, Dordrecht, 1987).
- ¹²J. C. Mallinson, *The Foundations of Magnetic Recording*, 2nd. ed. (Academic, San Diego, CA, 1993), p. 92.
- ¹³E. van de Riet and F. Rooseboom, *J. Appl. Phys.* **81**, 350 (1997).